Contribution from the Department of Chemistry,
Texas A&M University, College Station, Texas 77843

Synthesis and Molecular Structure of Two Members of a New Family of Zinc Organophosphates

Y. Ortiz-Avila, P. R. Rudolf, and A. Clearfield*

Received September 29, 1988

$Zn(O_3POC_2H_5)\cdot H_2O$ crystallizes in the orthorhombic space group *Pbca* with $a = 7.942$ (3) Å, $b = 20.554$ (5) Å, $c = 7.774$ (2) Å, $V = 1268.9$ (7) Å^3, and $Z = 8$; $Zn(O_3POC_2H_4NH_3)(O_2CCH_3)$ crystallizes in the same space group with $a = 9.655$ (14) Å, $b = 23.692$ (13) Å, $c = 7.934$ (7) Å, $V = 1815.9$ (31) Å^3, and $Z = 8$. Both compounds have layers formed by phosphate groups bridging the tetrahedral zinc atoms, which undulate perpendicular to the layer direction. The layers in the ethyl phosphate structure are centered at $y = {}^1/_4$ and ${}^3/_4$ and in the aminoethyl derivative at $y = 0$ and ${}^1/_2$. The spacing between successive layers is determined by the pendant groups: the ethyl group in the ethyl derivative and the acetate group in the amino compound. The amino groups fold back upon themselves to hydrogen-bond to the acetate groups. Hydrogen bonding produces sheetlike structures with only van der Waals forces holding adjacent sheets together.

Introduction

Over the past decade the number of known layered metal phosphonates has been on the increase. Phosphonates of group IV metals have been extensively characterized by Alberti et al.,[1] Dines and co-workers,[2] and Clearfield.[3] Vanadium(IV) has also been found to form a family of layered vanadyl phosphonates.[4] A large group of divalent metal phenylphosphonates has been described by Cunningham et al.,[5] but they were not able to carry out X-ray structure determinations. Recently the structures of two members of the series, $Mn(O_3PC_6H_5)\cdot H_2O$[6] and $Zn(O_3PC_6H_5)\cdot H_2O$,[7] have been solved. The metal atoms in these compounds are octahedrally coordinated within the layer by phosphonate oxygens while the phenyl groups fill the interlamellar space alternatively above and below the layer. Each phosphonate group coordinates to four zinc atoms. Two of the phosphonate oxygens chelate a zinc atom, and at the same time these oxygens act as electron-pair donors to bridge to two other zinc atoms. The third oxygen serves to bridge these zigzag chains into layers. The final coordination site is occupied by water. This layered arrangement is the same as that found in the inorganic phosphates of the type $M^IM^{II}PO_4\cdot H_2O$, where M^{II} is Fe, Ni, and Cu and M^I is an alkali-metal or ammonium ion.[8,9]

We subsequently attempted to synthesize alkyl phosphates with the same structure. Instead we were able to obtain crystals of four-coordinate compounds and report on these findings at this time.

Experimental Section

Preparation of $Zn(O_3POCH_2CH_3)\cdot H_2O$. A 30-mL amount of 0.1 M ethyl phosphate (K&K) solution was added to 20 mmol of zinc acetate dihydrate to obtain a clear solution. The solution was kept at 40 ± 2 °C for 2 weeks, during which time small crystals appeared. The crystals were recovered by filtration and washed with three 10-mL portions of distilled water. The yield was 0.18 g or 29% based upon the ethyl phosphate recovered.

Preparation of $Zn(O_3POCH_2CH_2NH_3)(O_2CCH_3)$. A 5-g amount of $BaO_3POCH_2CH_2NH_2$, prepared as described previously,[10] was dissolved in 50 mL of water and passed through a strong acid cation exchange resin (Dowex 50) to liberate the free acid. The pH of the treated solution was 2.11. A 20-mL portion of 1 M zinc acetate solution was added to the acid dropwise with stirring. A portion of solid precipitated during this addition, which was filtered off and discarded. The clear filtrate was kept in a constant-temperature bath at 30 ± 1 °C for 10 days. Crystals slowly formed during this time, and these were collected, washed, and air-dried; yield 1.2 g or 25% based on the barium phosphate.

X-ray Single-Crystal Measurements. All measurements were made on a Rigaku AFC5R diffractometer using an RU200 12-kW rotating-anode generator with graphite-monochromated Mo Kα radiation ($\lambda_{K\alpha}$ = 0.71069 Å). Experimental conditions and crystallographic parameters for both compounds are presented in Table I. In both cases, data were collected at ambient temperature. Crystals were mounted on glass fibers in a random orientation. The diameter of the incident beam collimator was 0.5 mm and the crystal to detector distance 22.5 cm. MSC/AFC control software[11] was used for the data collection.

Intensities were measured as $C - {}^1/_2(t_c/t_b)(b_1 + b_2)$, where C = total number of counts, t_c = time spent counting peak intensity, t_b = time spent counting one side of background, b_1 = high-angle background counts, b_2 = low-angle background counts; the intensity error $\sigma(F^2) = (C + {}^1/_4(t_c/t_b)^2(b_1 + b_2) + PI)^2)^{1/2}$, where I is the intensity and P is the factor that downweights strong reflections, equal to 0.05. All calculations in the structure solution and refinement were made by using the TEXSAN crystallographic software package[12] on a MicroVAX-II-based system.

Table I. Collected Experimental and Crystallographic Parameters

	ethyl phosphate	aminoethyl phosphate
empirical formula	$ZnPO_5C_2H_7$	$ZnPO_6NC_4H_{10}$
fw	207.43	264.48
color, form	colorless needles	colorless parallelepiped
cryst dimens, mm	0.05 × 0.05 × 0.15	0.20 × 0.20 × 0.10
cryst syst	orthorhombic	orthorhombic
space group	*Pbca*	*Pbca*
a, Å	7.942 (3)	9.655 (14)
b, Å	20.554 (5)	23.692 (13)
c, Å	7.774 (2)	7.934 (7)
V, Å^3	1268.9 (7)	1815.9 (31)
Z	8	8
radiation	Mo Kα, λ = 0.71069 Å	
ρ_{calc}, g cm^{-3}	2.17	1.94
μ(Mo Kα), cm^{-1}	29.42	41.63
transmission coeff	0.87–1.0 (ψ scan)	0.90–1.03 (DIFABS)
$R(F_o)$	0.067	0.068
$R_w(F_o)$	0.106	0.082
S	2.30	1.45
temp, °C	24 ± 1	24 ± 1

(1) (a) Alberti, G.; Constantino, U.; Alluli, S.; Tomassini, J. *J. Inorg. Nucl. Chem.* **1978**, *40*, 1113. (b) Alberti, G.; Constantino, U.; Giovagnotti, M. L. L. *J. Chromatogr.* **1979**, *180*, 45.
(2) (a) Dines, M. B.; DiGiacomo, P. *Inorg. Chem.* **1981**, *20*, 92. (b) Dines, M. B.; DiGiacomo, P.; Callahan, K. P.; Griffith, P. C.; Lane, R.; Cooksey, R. E. In *Chemically Modified Surfaces in Catalysis and Electrocatalysis*; Miller, J., Ed.; ACS Symposium Series 192; American Chemical Society: Washington, DC, 1982; p 223. (c) Dines, M. B.; Griffith, P. C. *Inorg. Chem.* **1983**, *22*, 567. (d) Dines, M. B.; Cooksey, R. E.; Griffith, P. C. *Inorg. Chem.* **1983**, *22*, 1003. (e) Dines, M. B.; Griffith, P. C. *Polyhedron* **1983**, *2*, 607.
(3) Clearfield, A. In *Design of New Materials*; Clearfield, A., Cocke, D. A., Eds.; Plenum: New York, 1986; p 121.
(4) Johnson, J. W.; Jacobson, A. J.; Brody, J. F.; Lewandowski, J. T. *Inorg. Chem.* **1984**, *23*, 3842.
(5) Cunningham, D.; Hennelly, P. J. D.; Deeney, T. *Inorg. Chim. Acta* **1968**, *37*, 95.
(6) Cao, G.; Lee, H.; Lynch, V. M.; Mallouk, T. E. *Solid State Ionics* **1988**, *26*, 63.
(7) Martin, K.; Squattrito, P. J.; Clearfield, A. *Inorg. Chim. Acta* **1989**, *155*, 7.
(8) Durif, A.; Averbuch-Pouchot, M. T. *Bull. Soc. Fr. Mineral. Cristallogr.* **1968**, *91*, 495.
(9) Ivananov, Yu. A.; Egorov-Tismenko, Yu. K.; Simonov, M. A.; Belov, N. V. *Sov. Phys.—Crystallogr. (Engl. Transl.)* **1975**, *19*, 665; **1977**, *22*, 97.
(10) Cherbuliez, E.; Rabinowitz, J. *Helv. Chim. Acta* **1956**, *39*, 1455.
(11) "CONTROL automation for Rigaku single crystal diffractometers"; Molecular Structure Corp.: College Station, TX, 1986 (revised 1988).
(12) "TEXSAN Structure Analysis Package"; Molecular Structure Corp.: College Station, TX, 1985 (revised 1988).

* To whom correspondence should be addressed.

0020-1669/89/1328-2137$01.50/0

Table II. Positional and Equivalent Isotropic Thermal Parameters

atom	*x*	*y*	*z*	*B*(eqv),[a] Å²
	(a) $ZnO_3POC_2H_5 \cdot H_2O$			
Zn	0.7181 (4)	0.2036 (1)	0.1661 (4)	1.3 (1)
P	0.849 (1)	0.1677 (4)	0.523 (1)	1.2 (3)
O1	0.796 (2)	0.2937 (8)	0.181 (2)	1.9 (7)
O2	0.702 (2)	0.1669 (8)	0.395 (2)	1.3 (8)
O3	0.506 (2)	0.1929 (7)	0.055 (2)	1.5 (8)
O4	0.881 (2)	0.0940 (9)	0.582 (2)	2.0 (9)
O10	0.876 (2)	0.1628 (8)	0.004 (2)	1.3 (8)
C5	0.746 (3)	0.058 (1)	0.658 (4)	2 (1)
C6	0.811 (4)	−0.009 (1)	0.685 (4)	3 (2)
H10	0.8743	0.1244	−0.0041	1.5
H11	0.9594	0.1760	0.1183	1.5
H12	0.7139	0.0768	0.7651	2.7
H13	0.6510	0.0572	0.5834	2.7
H14	0.7255	−0.0351	0.7351	4.0
H15	0.8432	−0.0269	0.5773	4.0
H16	0.9057	−0.0074	0.7592	4.0
	(b) $ZnO_3POC_2H_4NH_3 \cdot O_2CCH_3$			
Zn	0.0936 (2)	0.0693 (1)	0.1710 (2)	2.00 (8)
P	−0.2019 (4)	0.0339 (3)	0.0544 (5)	2.0 (2)
O1	−0.1099 (8)	0.0652 (6)	0.173 (1)	2.3 (5)
O2	0.161 (1)	0.0246 (6)	−0.015 (1)	2.5 (6)
O3	0.1488 (9)	0.0366 (6)	0.387 (1)	2.0 (5)
O4	−0.196 (1)	0.0650 (6)	−0.125 (1)	3.1 (6)
O5	0.173 (1)	0.1416 (6)	0.105 (1)	3.0 (7)
N	−0.079 (1)	0.0905 (7)	−0.436 (2)	3.7 (8)
C1	−0.150 (2)	0.120 (1)	−0.153 (2)	4 (1)
C2	−0.044 (2)	0.123 (1)	−0.276 (3)	5 (1)
O6	0.090 (2)	0.1680 (7)	0.352 (2)	5.5 (8)
C3	0.155 (2)	0.178 (1)	0.224 (3)	4 (1)
C4	0.225 (3)	0.234 (1)	0.204 (3)	8 (2)
H1	−0.1609	0.1058	−0.4840	4.4
H2	−0.0049	0.0938	−0.5137	4.4
H3	−0.0936	0.0519	−0.4091	4.4
H4	−0.2255	0.1426	−0.1905	5.1
H5	−0.1147	0.1352	−0.0506	5.1
H6	0.0383	0.1070	−0.2298	5.5
H7	−0.0280	0.1610	−0.3052	5.5
H8	0.2866	0.2399	0.2947	9.5
H9	0.2717	0.2353	0.1005	9.5
H10	0.1549	0.2630	0.2064	9.5

[a] $B(\text{eqv}) = {}^4/_3[a^2\beta_{11} + b^2\beta_{22} + c^2\beta_{33} + 2ab(\cos\alpha)\beta_{12} + 2ac(\cos\beta)\beta_{13} + 2bc(\cos\alpha)\beta_{23}]$.

Neutral-atom scattering factors were taken from Cromer and Waber.[13] Anomalous dispersion effects[14] were included in F; the anomalous dispersion terms $\Delta f'$ and $\Delta f''$ were those of Cromer.[15]

$ZnO_3POC_2H_5 \cdot H_2O$. Cell parameters were obtained from least-squares refinement using setting angles of 22 accurately refined reflections in the range $25.55 < 2\theta < 30.08°$ and corresponded to an orthorhombic cell with $a = 7.942$ (3) Å, $b = 20.554$ (5) Å, $c = 7.774$ (2) Å. Systematic absences of $0kl$ ($k = 2n + 1$), $h0l$ ($l = 2n + 1$), and $hk0$ ($h = 2n + 1$), followed by successful solution and refinement of the structure, determined the space group as *Pbca* for $Z = 8$. Data were collected in AUTO mode by using the 2θ–ω scan technique to a maximum 2θ value of 50.0°. ω scans of several intense reflections, made prior to data collection, had an average width of 1.45°, which experimentally determined the scan value $A = 1.52°$ in ω with the takeoff angle of 6.0°. Scans of $(1.52 + 0.30 \tan\theta)°$ were made at a speed of 8.0°/min in ω. The weak reflections ($I < 10.0\sigma(I)$) were rescanned a maximum of twice, and the counts were accumulated to assure good counting statistics. Stationary background counts were recorded on each side of the reflection. The ratio of peak counting time to background counting time was 2:1. A total of 1342 unique reflections were measured from 0 to 50° in 2θ. The intensities of three representative reflections that were measured after every 150 reflections remained constant throughout data collection, indicating crystal and electronic stability. No decay correction was applied.

An empirical absorption correction, based on azimuthal scans of three reflections, was applied, which resulted in transmission factors ranging from 0.87 to 1.00. The data were corrected for Lorentz and polarization effects but not extinction.

The structure was solved by direct methods.[16] The non-hydrogen atoms were refined anisotropically. Hydrogen atoms were included in the structure factor calculation in idealized positions ($d_{C-H} = 0.95$ Å) and were assigned isotropic thermal parameters that were 20% greater than the B(eqv) value of the atom to which they were bonded. The final cycle of full-matrix least-squares refinement[17] was based on 527 observed reflections ($I > 3.00\sigma(I)$) and 82 variable parameters and converged (largest parameter shift was 1.47 times its esd) with unweighted and weighted agreement factors

$$R = \sum||F_o| - |F_c||/\sum|F_o| = 0.067$$

$$R_w = [\sum w(|F_o| - |F_c|)^2/\sum wF_o^2]^{1/2} = 0.106$$

The standard deviation of an observation of unit weight[18] was 2.3. The largest peak remaining in the final difference Fourier was 1.1 e/Å³.

$ZnO_3POC_2H_4NH_3 \cdot O_2CCH_3$. Soft, poorly diffracting crystals were cut to size and data collection parameters optimized for weak crystal diffraction. Cell parameters were based on accurately refined peaks in the range $10.05 < 2\theta < 20.50°$. Because of the broadness of individual reflections, data were collected by ω-step-scan methods with a fixed scan

Table III. Intramolecular Bond Distances (Å) and Angles (deg)

	(a) $ZnO_3POC_2H_5 \cdot H_2O$		
	Distances		
Zn–O3	1.90 (2)	P–O1	1.52 (2)
Zn–O2	1.94 (2)	P–O2	1.53 (2)
Zn–O1	1.96 (2)	P–O4	1.60 (2)
Zn–O10	1.97 (2)	O4–C5	1.44 (3)
P–O3	1.49 (2)	C5–C6	1.48 (3)
	Angles		
O3–Zn–O2	108.4 (8)	O1–P–O2	109 (1)
O3–Zn–O1	114.6 (7)	O1–P–O4	108 (1)
O3–Zn–O10	102.9 (8)	O2–P–O4	107 (1)
O2–Zn–O1	109.4 (7)	P–O1–Zn	122 (1)
O2–Zn–O10	117.7 (7)	P–O2–Zn	123 (1)
O1–Zn–O10	103.9 (7)	P–O3–Zn	166 (1)
O3–P–O1	112 (1)	C5–O4–P	119 (2)
O3–P–O2	112 (1)	O4–C5–C6	106 (2)
O3–P–O4	108 (1)		
	(b) $Zn(O_3POC_2H_4NH_3)(O_3CCH_3)$		
	Distances		
Zn–O2	1.93 (1)	P–O4	1.60 (1)
Zn–O5	1.95 (1)	O4–C1	1.40 (2)
Zn–O3	1.96 (1)	O5–C3	1.29 (2)
Zn–O1	1.968 (9)	O6–C3	1.22 (2)
P–O2	1.47 (1)	C3–C4	1.49 (3)
P–O1	1.49 (1)	N–C2	1.52 (2)
P–O3	1.52 (1)	C1–C2	1.42 (2)
	Angles		
O2–Zn–O5	98.4 (5)	O3–P–O4	106.6 (6)
O2–Zn–O3	111.3 (5)	P–O1–Zn	127.8 (6)
O2–Zn–O1	108.3 (4)	P–O2–Zn	140.0 (8)
O5–Zn–O3	118.4 (5)	P–O3–Zn	123.0 (6)
O5–Zn–O1	116.0 (5)	C1–O4–P	126 (1)
O3–Zn–O1	104.1 (4)	C3–O5–Zn	110 (1)
O2–P–O1	116.0 (7)	O4–C1–C2	112 (2)
O2–P–O3	111.2 (8)	C1–C2–N	113 (2)
O2–P–O4	103.7 (7)	O6–C3–O5	123 (2)
O1–P–O3	110.5 (6)	O6–C3–C4	119 (2)
O1–P–O4	108.2 (7)	O5–C3–C4	117 (2)

(13) Cromer, D. T.; Waber, J. T. *International Tables for X-ray Crystallography*; Kynoch Press: Birmingham, England, 1974; Vol. IV, Table 2.2A.
(14) Ibers, J. A.; Hamilton, W. C. *Acta Crystallogr.* **1964**, *17*, 781.
(15) Cromer, D. T. *International Tables for X-ray Crystallography*; Kynoch Press: Birmingham, England, 1974; Vol. IV, Table 2.3.1.
(16) Direct methods: (a) Gilmore, C. J. "MITHRIL—a computer program for the automatic solution of crystal structures from X-ray data"; University of Glasgow: Glasgow, Scotland, 1983. (b) Beirskens, P. T. "DIRDIF: Direct Methods for Difference Structures-an automatic procedure for phase extension and refinement of difference structure factors"; Technical Report 1984/1; Crystallograpical Laboratory: Toernooiveld, 6526 ED Nijmegen, The Netherlands, 1984.
(17) The function minimized in the least-squares analysis was $\sum w(|F_o| - |F_c|)^2$, where $w = 4F_o^2/\sigma^2(F_o^2)$, $\sigma^2(F_o^2) = [S^2(C + R^2B) + (PF_o^2)^2]/(Lp)^2$, S = scan rate, C = total integrated peak count, R = ratio of scan time to background counting time, B = total background count, Lp = Lorentz–polarization factor, and P = P factor.
(18) The standard deviation of an observation of unit weight is expressed as $[\sum w(|F_o| - |F_c|)^2/(N_o - N_v)]^{1/2}$, where N_o = number of observations and N_v = number of variables.

Table IV. Possible Hydrogen-Bonding Contacts

atom 1	atom 2	dist, Å	direction
	(a) $Zn(O_3POCH_2CH_3)\cdot H_2O$		
O2	O10	2.71 (2)	*xz*
O3	O10	3.18 (2)	*xz*
	(b) $Zn(O_3POCH_2CH_2NH_3)(O_2CCH_3)$		
O1	N	3.17 (2)	*z*
O2	N	2.98 (2)	*x*
O3	N	2.91 (2)	*xz*
O4	N	2.78 (2)	*z*
O5	N	3.00 (2)	*xz*
O6	N	2.98 (2)	*xz*

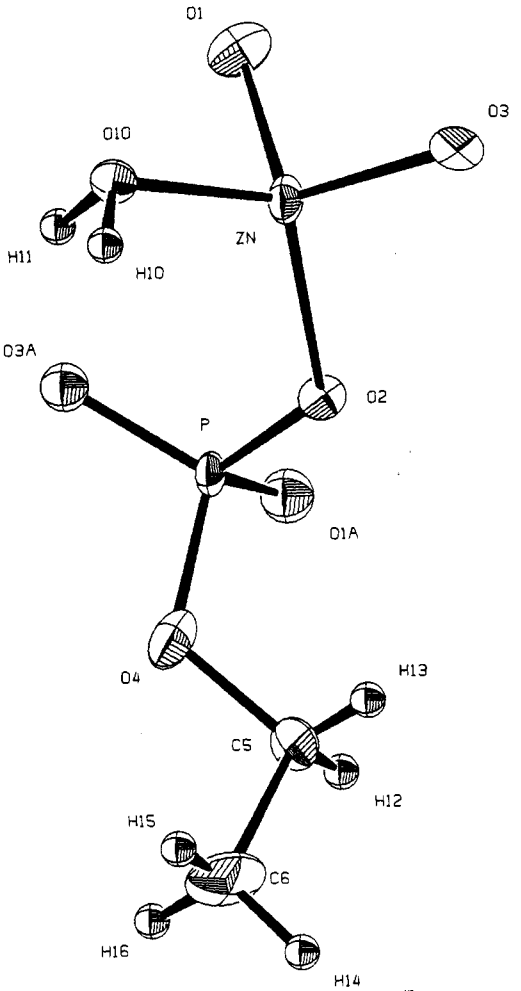

Figure 1. Molecular representation and atom-numbering scheme for zinc ethyl phosphate hydrate.

width of 2° in ω and a speed of 4°/min in ω. Scans were time-sliced to 32 steps/scan. No discreet background measurement was made. The step-scan data were then processed by on-the-fly Lehmann–Larsen processing methods for background determination, signal to noise optimization, and peak modeling. Data processing, as before, on 1887 unique data collected to 50° in 2θ again yielded systematic absences consistent with space group *Pbca* for $Z = 8$ and cell parameters $a = 9.655$ (14) Å, $b = 23.692$ (13) Å, and $c = 7.934$ (7) Å.

The structure was solved by auto-Patterson interpretation, which located the Zn atom. The additional atoms were then found by using DIRDIF.[16b] Non-hydrogen atoms were refined anisotropically; hydrogens were included as fixed contributions in the manner described previously. No suitable ψ-scan reflections were available with this crystal, so an absorption correction based on the statistical 2θ dependence of F_o versus F_c (DIFABS) was calculated after full isotropic refinement. The final cycle of least-squares refinement using 752 observations with $I > 2\sigma(I)$ and 118 variables converged with a maximum parameter shift of 0.4 of its esd. Residuals were $R = 0.068$, $R_w = 0.082$, and $S = 1.45$. The largest peak remaining in the final Fourier difference map was 1.3 e/Å^3.

Final positional and equivalent isotropic thermal parameters are given in Table II, bond distances and angles in Table III, and hydrogen-bonding contacts in Table IV.

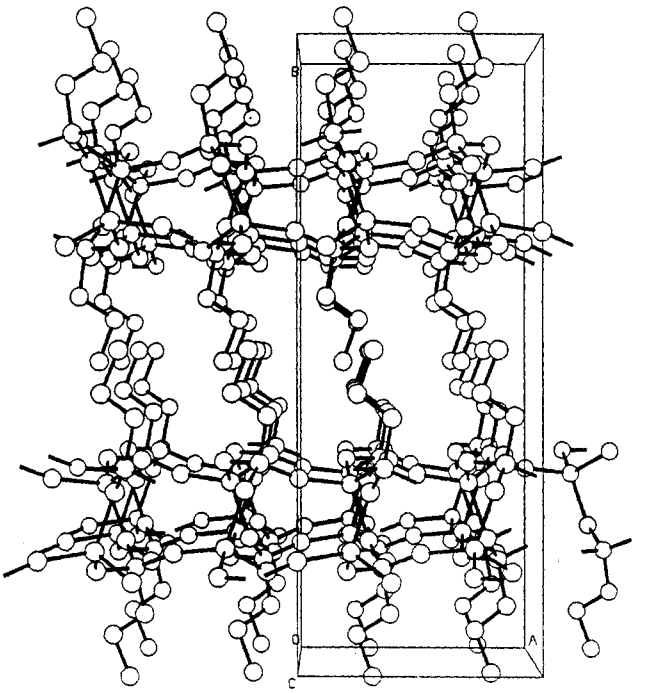

Figure 2. Layer arrangement in the cell of zinc ethyl phosphate hydrate projected along *c*. The ethyl groups form a herringbone packing array between the layers.

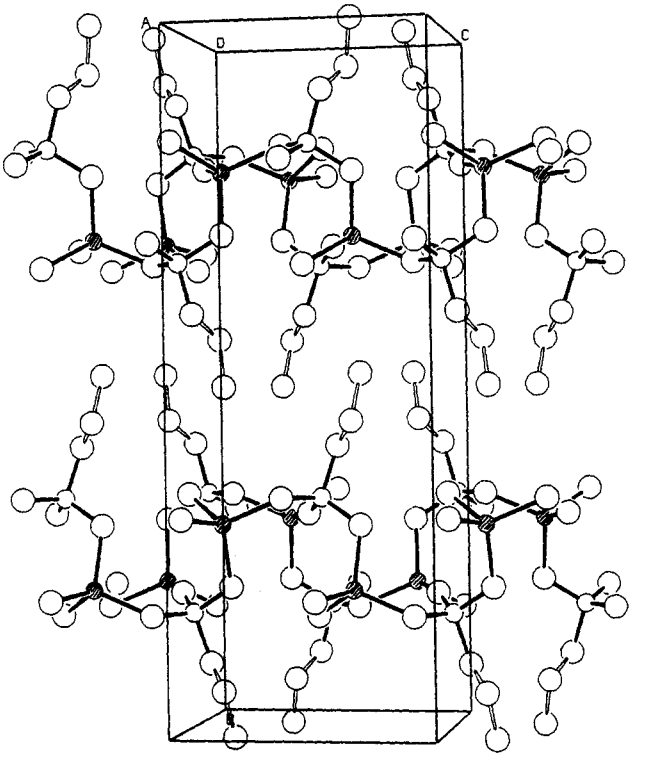

Figure 3. View of zinc ethyl phosphate hydrate as seen down the *a* axis. The heavy lines outline the Zn and P tetrahedra, while the zinc atoms are designated with stripes.

Anisotropic thermal parameters and structure factors are available in Tables SI and SII for $Zn(O_3POCH_2CH_3)\cdot H_2O$ and Tables SIII and SIV for $Zn(O_3POC_2H_4NH_3)(O_2CCH_3)$, respectively (see supplementary material).

Results

Figure 1 shows the building block for the $Zn(O_3POC_2H_5)\cdot H_2O$ structure, while the cell packing is shown in Figure 2. The building unit and cell packing for $Zn(O_3POC_2H_4NH_3)(O_2CCH_3)$ are shown in Figures 4 and 5, respectively. Both compounds contain tetrahedrally coordinated Zn atoms. In the ethyl phos-

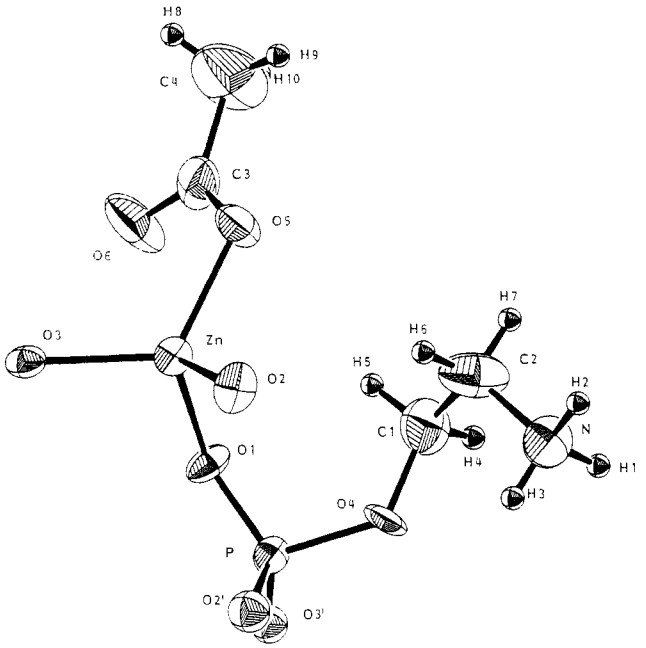

Figure 4. Molecular representation and atom-numbering scheme in zinc 2-aminoethyl phosphate acetate.

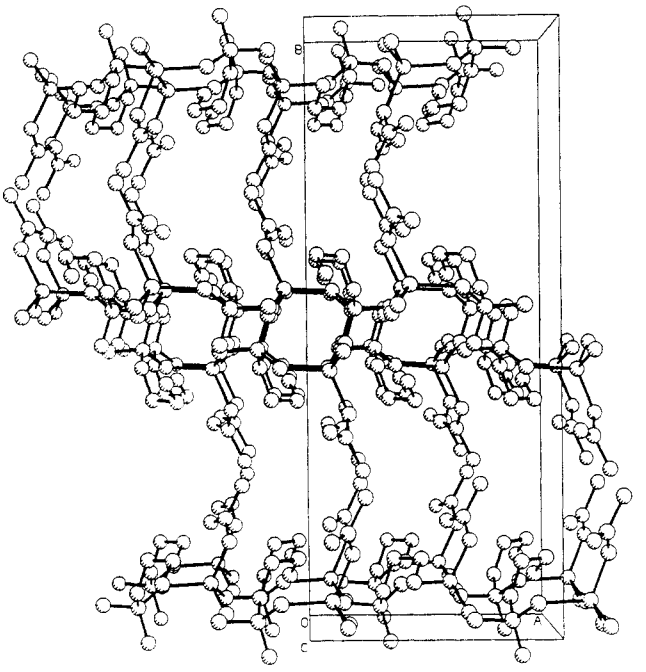

Figure 5. Layer arrangement and unit cell packing of zinc 2-aminoethyl phosphate acetate as seen down the *c* axis. The interlayer distance is packed with interpenetrant acetate groups.

phate compound three of the four Zn–O bonds are to different bridging phosphate groups and the fourth bond is with the water molecule oxygen. The linkage is such that two Zn–O–P links are in the *ac* plane, forming chains of zinc and oxygen atoms along the *a* direction. The third phosphate oxygen is in the *b* direction and serves to link chains together, forming a layer. One row of zinc atoms parallel to the *a* direction is at $0.2036y$, and a second row is at $0.2964y$. Thus, in projection (Figure 2) it appears as though rings are formed. Instead, the layer undulates from the lower to higher positions in alternate rows with the layers centered at $y = 0.25$ and 0.75. This is shown in Figure 3, where the view is now down the *a* axis. The heavy lines outline the zinc and phosphorus octahedra. The space between the layers (Figure 2) is filled with herringbone-packed ethyl groups. The distance between methyl carbon atoms in the *c* direction is about 4 Å, which is equal to the distance required by van der Waals radii for a

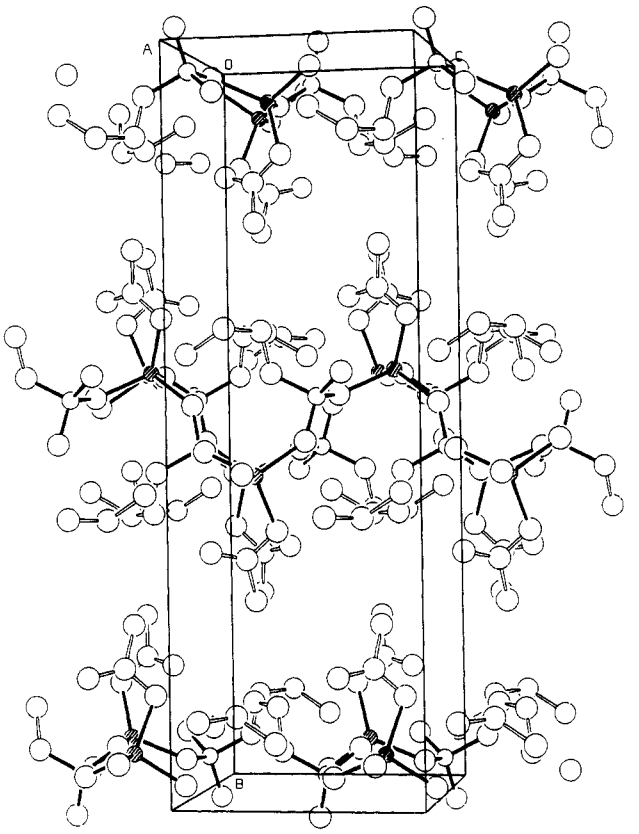

Figure 6. Schematic view of zinc 2-aminoethyl phosphate acetate as seen down the *a* axis. The heavy lines outline the Zn and P tetrahedra, while the Zn atoms are designated with stripes.

methyl group. In the *a* direction, this distance is about 0.1 Å longer, so essentially the alkyl groups are tightly packed rather than having spaces between them as shown in Figures 2 and 3.

$Zn(O_3POC_2H_4NH_3)(O_2CCH_3)$ has a layer arrangement similar to that of the ethyl phosphate compound. The layers, however, are at $y = 0.0$ and $y = 0.5$ (Figure 5). One oxygen of the acetate ion bonds to zinc and takes the place occupied by water in the zinc ethyl phosphate. The acetate carbons then extend in the *b* direction much as the ethyl groups do in the zinc ethyl phosphate and thus determine the spacing of the layers in that direction. The aminoethyl group is then twisted back around on itself so as to form the maximum number of hydrogen bonds (Table IV). There are no hydrogen bonds between layers in the *b* direction so that the sheet packing is controlled by van der Waals forces. This arrangement leaves small gaps between acetate groups in the *z* direction and between the layers because of the conformation of the aminoethyl groups. These gaps are clearly seen in Figure 6, a view of the layers down the *a* axis. Since the layers are only lightly bound together by van der Waals forces, the poor quality of the aminoethyl crystals, as evidenced by the large mosaic spread, along with the softness and weakly diffracting character is therefore a function of the way adjacent layers pack. However, the acetate groups are tightly packed in the *xz* plane. The zinc–oxygen distances range from 1.90 (2) to 1.97 (2) Å with the maximum deviation from a tetrahedral angle of ca. 9°. The shorter *a* axis in the ethyl material yields a more distorted structure with a P–O3–Zn angle of 166°, 26° more than in the less distorted aminoethyl compound.

Discussion

As mentioned in the Introduction, Mallouk et al.[6] prepared phenylphosphonates of transition metals of the type described in the Introduction and also a family of a layered alkylphosphonates of Mg, Mn, and Zn.[6,19] These alkylphosphonates have the same

(19) Cao, G.; Lee, H.; Lynch, V. M.; Mallouk, T. E. *Inorg. Chem.* **1988**, *27*, 2781.

layer structure as the phenylphosphonates and therefore have octahedrally coordinated Zn atoms rather than the tetrahedra as described for the ethyl phosphate derivative reported here. It is interesting to note that the layered zinc ethyl phosphonate has a *b* axis which is almost half as large (10.14 Å)[19] as the *b* axis of the zinc ethyl phosphate reported here. The interlamellar space is fully packed in both the zinc ethylphosphonate and ethyl phosphate. The distance between adjacent methyl groups in the latter compound is 4.02–4.10 Å, which is close to the required van der Waals distance. However, in the ethyl phosphate O2 and phosphorus have very similar *b* parameters, while the OC_2H_5 groups tilt in the *c* direction. Both of these conditions shorten the total extension in the *b* direction (perpendicular to the layers) of the ethyl phosphate groups to a value of 4.37 Å. If we add half the distance of the layer thickness (0.77 Å) to this value, we obtain the requisite distance of 5.14 Å. The comparable extension of the pendant groups in the ethylphosphonate, including the van der Waals distance between the ethyl groups in adjacent layers, is very similar, being half the *b*-axis distance or 5.07 Å.

It is of interest now to see if organic phosphates of group II metals can form layered compounds similar to the layered phosphonates. Such work is in progress.

Acknowledgment. This work was supported by the Army Research Office (Grant No. DAAG29-85-K-0124) and the Robert A. Welch Foundation (Grant No. A673), for which grateful acknowledgment is made. The diffractometer facility was made possible by DOD Grant No. 00014-86-G-0194.

Registry No. $Zn(O_3POCH_2CH_3)\cdot H_2O$ (coordination compound entry), 120313-05-5; $Zn(O_3POCH_2CH_2NH_3)(O_2CCH_3)$, 120313-06-6; $BaO_3POCH_2CH_2NH_2$, 63441-18-9; $Zn(O_3POCH_2CH_3)\cdot H_2O$ (salt entry), 120313-04-4; ethyl phosphate, 1623-14-9; zinc acetate, 557-34-6.

Supplementary Material Available: Tables SI and SIII, listing thermal parameters for zinc ethyl phosphate hydrate and zinc 2-aminoethyl phosphate acetate (2 pages); Tables SII and SIV, listing calculated and observed structure factors (10 pages). Ordering information is given on any current masthead page.

Contribution from the Dipartimento di Chimica and Dipartimento di Scienza della Terra, Sezione Cristallografia, Università di Perugia, 06100 Perugia, Italy

Exchange Coupling in $Cu_2L_2Cl_2\cdot 2CH_3OH$ (LH = 8-(Salicylideneamino)quinoline), a New Compound with a Temperature-Dependent Structure[1]

B. Chiari, O. Piovesana,* T. Tarantelli, and P. F. Zanazzi

Received June 29, 1988

The synthesis, room-temperature crystal and molecular structure, and magnetic properties are reported for the new compound $Cu_2L_2Cl_2\cdot 2CH_3OH$, where L^- is the anion of 8-(salicylideneamino)quinoline:

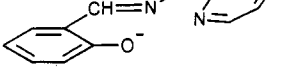

The compound, $Cu_2C_{34}H_{30}N_4O_4Cl_2$, crystallizes in the triclinic space group $P\bar{1}$. Cell dimensions are as follows: a = 11.951 (3) Å, b = 8.943 (2) Å, c = 8.111 (2) Å, α = 112.02 (2)°, β = 107.45 (2)°, γ = 79.20 (2)°, Z = 1. The structure was solved at room temperature by direct methods and refined to an R value of 0.038 (R_w = 0.039), for 213 parameters and 1914 observed reflections. The structure consists of binuclear molecules and uncoordinated methanol molecules of solvation. The binuclear molecule exhibits a centrosymmetric, parallel-planar structure in which each copper atom shows distorted (4 + 1) square-pyramidal coordination. The long, apical bond is to the basal chlorine atom of the other copper atom. Therefore, each bridging chlorine simultaneously occupies an in-plane coordination site on one copper(II) ion and an apical site on the other copper(II) ion. The dimeric units in the structure are well separated from one another. In particular, the oxygen atom of the solvent molecule is not involved in any bridging between dimers. Surprisingly, in light of the dimeric structure of the compound at room temperature, the variable-temperature magnetic susceptibility data between 4.2 and 50 K cannot be reproduced by the dimer exchange model. A precise description of the experimental data can instead be achieved with use of the Heisenberg model for isotropic antiferromagnetic exchange in linear chains, with J = −9.30 cm^{-1} and g = 2.08. The noncongruent structural and magnetic properties of the compound are briefly discussed.

Introduction

The study of magnetic exchange in solids is mainly aimed toward relating the observed magnetic properties of a material to the nature of its chemical constituents and the way in which these are bound together to form the crystal lattice.[2]

A common experimental approach for such a study is to correlate low-temperature magnetic susceptibility data (from which the sign and magnitude of the exchange coupling constant, J, are generally deduced) with X-ray results obtained at room temperature.

This approach obviously relies on the dual expectation that the prominent structural features of a given substance dictate its magnetic properties in the whole temperature region which is of interest and that variations in structure with temperature can be neglected. As an example, compounds having zero-dimensional (clusters) or one-dimensional (chains) structures at room temperature are expected to obey theoretical models whose statistics treats only spins interacting in the individual structural cluster or chain.

* To whom correspondence should be addressed at the Dipartimento di Chimica, Università di Perugia.

(1) Exchange Interaction in Multinuclear Transition-Metal Complexes. 13. Part 12: Chiari, B.; Piovesana, O.; Tarantelli, T.; Zanazzi, P. F. *Inorg. Chem.* **1988**, *27*, 4149–4153.

(2) For reviews see: (a) *Magneto-Structural Correlations in Exchange Coupled Systems*; Reidel: Dordrecht, The Netherlands, 1985. (b) Hatfield, W. E. *Comments Inorg. Chem.* **1981**, *1*, 105. (c) O'Connor, C. J. *Prog. Inorg. Chem.* **1982**, *29*, 203. (d) Kahn, O. *Comments Inorg. Chem.* **1984**, *3*, 105; *Angew. Chem., Int. Ed. Engl.* **1985**, *24*, 834. (e) Melnic, M. *Coord. Chem. Rev.* **1982**, *42*, 259. (f) Cairns, C. J.; Busch, D. H. *Coord. Chem. Rev.* **1986**, *69*, 1. (g) Carlin, R. L. *Coord. Chem. Rev.* **1987**, *79*, 215. (h) Hatfield, W. D.; Estes, W. E.; Marsh, W. E.; Pickens, M. W.; ter Haar, L. W.; Weller, R. R. In *Extended Linear Chain Compounds*; Miller, J. S., Ed.; Plenum: New York, 1983; Vol. 3. (i) Carlin, R. L.; de Jongh, L. J. *Chem. Rev.* **1986**, *86*, 659.

0020-1669/89/1328-2141$01.50/0